



Stability analysis of unbraced steel storage racks: discussions an alternatives

Maria A. Branquinho¹, Luiz C.M. Vieira Jr.², Maximiliano Malite³

Abstract

This paper aims to evaluate simplified methods used to perform frame stability analysis; effective length method and direct analysis method are compared as alternative to analyze irregular unbraced steel pallet racks. Steel storage racks are composed by: perforated thin-walled steel profiles, beam-to-column hook-in connectors, and base connections; the structural analysis of these systems shall consider semi-rigid connection between the elements and global, local, and distortional buckling in perforated profiles. Herein, the direct analysis is carried out according to AISC and AISI design standards, whereas the effective length analysis is performed according to the steel rack design specification. Advanced analysis is carried out for typical unbraced steel storage rack using finite element model and beam elements; geometrical and material nonlinearities, as well as initial geometric imperfections, semi-rigid beam-to-column, and base connections were taken in account. Comparative analysis indicates that the direct analysis method is an advantageous alternative to the effective length method. Since beam element models are not able to predict local and distortional buckling, we, herein, propose the use of lattice models to take these buckling modes in account while still only using beam and truss elements in the analysis. The results obtained using lattice models are shown to be an effective alternative to analyze large steel frames with complex interaction between the elements and subjected to local and distortional buckling.

1. Introduction

Steel storage pallet racks are attracting considerable market interest by allowing the storage of large quantities of products in limited spaces with high strength-to-weight ratio. Usually, steel storage racks are composed by perforated cold-formed steel (CFS) profiles, semi-rigid beam-to-column hook-in connectors (BCC), semi-rigid base-plate connections and semi-rigid splices. The mechanical behavior of racks is different in down-aisle direction and in cross-aisle direction as shown in Fig. 1. In down-aisle direction, the rack is an unbraced frame and, therefore, the behavior of the components (column bases, BCC, columns strength) is critical to the stability of the frame. On the other hand, in cross-aisle direction, the racks are braced frames and their mechanical behavior is less complex.

¹ Ph.D. student, São Carlos School of Engineering, University of São Paulo, <maria_branquinho@yahoo.com.br>

² Professor, School of Civil Engineering, Architecture and Urban Design, University of Campinas, <luizvieirajr@gmail.com >

³ Titular Professor, São Carlos School of Engineering, University of São Paulo, <max.malite@gmail.com >

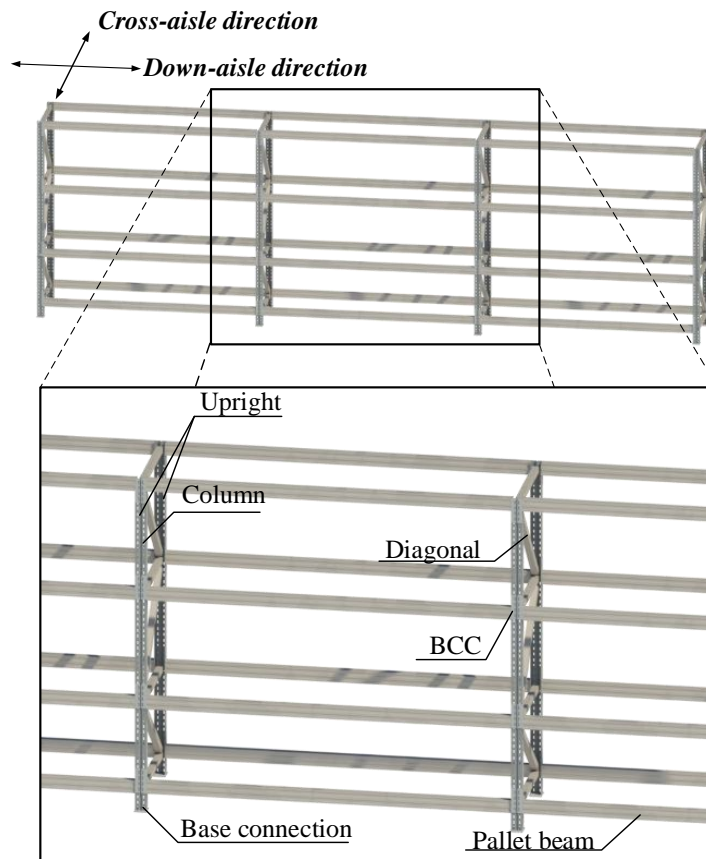


Figure 1: Type of steel storage pallet rack.

The plane analysis and design of racks in down-aisle direction can be carried out by two main simplified design methods: direct analysis method (or notional load method) and effective length method. ASCE 1997 indicates that both procedures are able to account for the several deleterious effects on member strength subject to compression or flexion-compression. However, they differ in how to consider these effects.

According to ASCE 1997, in the effective length method, the deleterious effects are accounted in column strength curve capacity that is present today in the American standards ANSI/AISI S100-16 and ANSI/AISC 360-16. Thus, each of the members subject to compression are designed using an effective length KL , with $K \neq 1$. On the other hand, in the direct analysis method, the actual member length is used for design, while artificially applying large imperfections in the system (which can be included by notional forces), in order to account for some destabilizing effects. Besides that, the direct analysis approach predicts a reduced stiffness in the structure depending on the value of the ratio of maximum second-order drift to maximum first-order drift. Thus, ASCE 1997 indicates that the direct analysis method accounts for the effects of residual stress, out-of-straightness of members (local imperfection), deviations in the design of connections, accidental loading eccentricities, and member-system interactions, affecting the term of the requesting moment in the M-N interaction expressions.

Despite the fact that the American standard for steel storage racks (RMI MH16.1:2012) specifies the effective length method for racks design, the standard allows the use of the direct analysis method presented in AISC and AISI. According RMI MH16.1:2008, where large lateral load requirements already exist (such as the higher seismic zones) a method employing the lateral load may dominate the stability considerations in the design and a K factor approach may not be required.

In the last decades, some studies have been published on design of steel storage pallet racks (Sarawit and Peköz 2006a, 2006b, Dória, Malite and Vieira Jr. 2013, Lavall et al. 2013, Rasmussen and Gilbert 2013, Trouncer and Rasmussen 2016a, 2016b). Sarawit and Peköz 2006b compared the effective length method and the direct analysis method for accuracy of the CFS rack design. The authors recommended that the direct analysis method be considered as an alternative for industrial steel storage rack design although local and distortional buckling failure modes were not considered in their study.

Dória, Malite and Vieira Jr. 2013 evaluated the impact of second-order effects in steel storage rack accounted by B_2 coefficient. The authors concluded that the B_2 multiplier considered in the ANSI/AISC 360-10, as a replacement for the second-order drift to first-order drift ratio, is not the best parameter to account the second-order effects in steel storage pallet racks.

Racks have high strength-to-weight ratio due their reduced wall thickness, i.e., the thin-walled cold-formed steel sections are prone to local and distortional buckling as well as overall buckling. Trounce and Rasmussen 2016a indicate that it is well understood that these cross-sectional deformations reduce the rigidity of the section, and hence amplify sway deflections and cause a redistribution of the internal forces in the structural frame. Trouncer and Rasmussen 2016a evaluated twelve full scale tests of ultra-light gauge steel storage rack frames in the Civil Engineering Structures Laboratory at the University of Sydney. One of the aims of this work was to present full scale tests to provide data for model verification purposes, in particular numerical models of advanced analysis.

Using results from the Trouncer and Rasmussen 2016a, Trouncer and Rasmussen 2016b calibrated finite element (FE) models to predict the strength of steel storage rack frames with increasingly slender cross-sections. The FE strengths were compared to Australian design strength predictions (AS 4084 and AS/NZS 4600) and conclusions were drawn about the extent to which current specifications are able to accommodate second order moments generated by local and/or distortional buckling modes.

Generally, the design standards of hot-rolled and CFS structures assume that the analysis is based on beam elements (Trouncer and Rasmussen 2016b). However, these elements assume that the cross-section of members is unchanged during the analysis and therefore neglect local and distortional cross-sectional deformations. The use of beam elements is suggested due to its low computational cost compared to the numerical analysis using shell elements – commonly used in CFS analyses (Cardoso and Rasmussen 2016). Herein, it is presented a novel method to analyze CFS profiles using one-dimensional elements: the lattice models.

Although steel racks are modular structures, there are irregular rack geometries depending on the type of products they store. In these cases, considerable attention must be paid depending on the types of loads being applied. The main goal of this paper is to evaluate the effectiveness of simplified design methodologies applied to irregular steel pallet racks subject to different loading conditions. Herein, the direct analysis is evaluated according to ANSI/AISI S100-16 whereas the effective length analysis is performed according to the steel rack design specification RMI MH16.1:2012. A rigorous frame analysis, advanced analysis, was developed to allow comparison of procedures. The numerical analysis are performed using Finite Element Method (FEM) to obtain the structure response through Abaqus 6.16 2016 commercial software. The study neglect effects of earthquake, wind and vertical impact loads; local and distortional buckling modes; perforated columns and effects of eventual cracking in BCC. Besides that, this research presents a new approach to analyze CFS based on lattice models. Herein, its applicability is showed in an isolated column.

This paper is organized into five sections. The first gives a brief overview of researches on design codes applied to racks. The second section presents the validation of advanced analysis developed. In the third section, an irregular rack subject to different loading conditions is evaluated by the direct analysis (AISI) and the effective length method (RMI); both results are compared to advanced analysis's results. A new numerical methodology based on lattice model is outlined in the fourth section. Conclusions are presented in the final section.

2. Advanced Analysis

The advanced analysis technique aims to present a more realistic numeric prediction of the effects of the loadings and the overall response of the structure and, therefore, allowing the comparison between design approaches. The validation of an advanced analysis was developed in steps. In each step, each component of the structure was validated. Cold-formed steel rack structure is known for its many peculiarities such as connections and cross-sectional type. The behavior of BCC is adopted as non-linear according Zhao et al. 2014 and the base connections was modeled with linear behavior defined according Sarawit and Peköz 2002. Additionally, local and distortional buckling modes, the perforated profiles and the splices were not studied in this paper. The validation of the advanced numerical analysis of the pallet racks is divided into two steps. Table 1 shows the steps and steel pallet rack features evaluated in each one.

Table 1: Steps of advanced analysis

	Steps	Steel pallet rack features				
		Steel structure	Out-of-straightness	Out-of-plumb	BCC	Base connection
Step I	Isolated simple-simple member	X	X			
	Isolated fixed-free member	X	X	X		
Step II	Vogel's portal frame	X	X	X		
	Beam-to-column connection (Zhao et al. 2014)	X			X	
	Base connection (Godley, Beale and Feng 1998; Sarawit and Peköz 2002)	X				X

The following subsections show some numerical results compiled through the model validation stage.

2.1 Step I: validation of isolated member

In this step one cross-section with two boundary conditions were evaluated: a simple-simple member and a fixed-free member. The columns studied is the Vogel' column HEB300 with length equal to 5000 mm, and E and f_{yd} equal to 20500 MPa and 235 MPa, respectively. Residual stresses were modeled according Galambos and Ketter 1959.

With these models, it is possible to evaluated the influence of only the out-of-straightness imperfection (with the simple-simple) and an additional out-of-plumb imperfection (fixed-free situation). Thus, the models consider geometric non-linearity, non-linearity in the material, residual stress and initial geometric imperfections. The resolution of the non-linear problem was carried out by the Riks method and the out-of-straightness imperfections was determined through previous elastic stability analysis. The model was composed by 3D beam elements, B32, in order to properly consider residual stress distribution. The B32 element has integration points in the flanges of section and not only in the web, unlike the 2D element B31. The mesh was defined with 12 elements in each column.

Fig. 2 and Fig. 3 show the numerical results of the isolated columns compared to the M-N interaction expression of ANSI/AISC 360-16. The present paper presents only the results of bending around strong axis because the numerical analysis aims to investigate the behavior of frames in down-aisle direction. The results show that the FEM model is able to predict satisfactorily the strength of an isolated member for various values of imperfection.

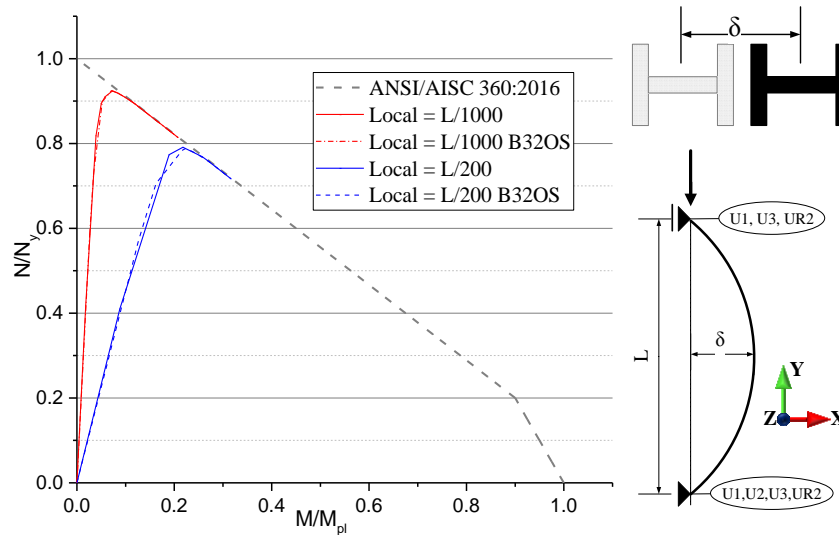


Figure 2: Results of simple-simple column

Fig.2 and Fig.3 show the details of the models on their boundary conditions. The simple-simple condition is defined by restricting the displacements in the X, Y and Z directions (U1, U2 and U3, respectively) and the twisting (UR2). Similarly, the fixed-free condition is modeled by restricting the displacements in the X, Y and Z directions and the rotations around X, Y and Z axes (UR1, UR2 and UR3, respectively).

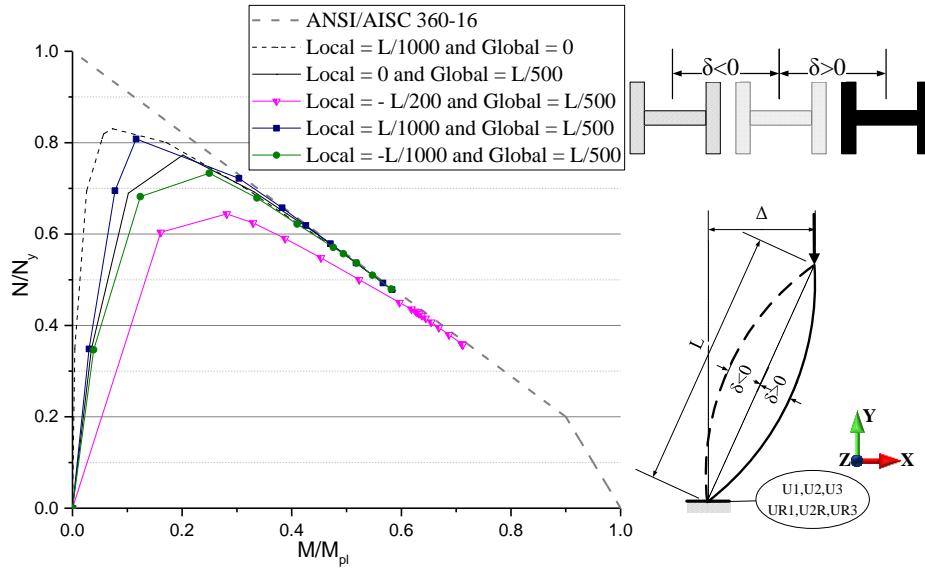


Figure 3: Results of fixed-free column

For the fixed-free case, Fig. 3 shows that positive local imperfections ($\delta > 0$) lead to greater strength when compared to null δ . On the other hand, negative values of local imperfection lead to lower strength values. ASCE 1997 reports the same conclusion for the isolated fixed-free columns. That is, the combination of local and global imperfections may provide restoring, greater strength than null δ , or destabilizing, lower strength than null δ , effects.

2.2 Step II: validation of frame and non-linear connections

The benchmark steel frame Vogel's portal frame was used to validate the FE model of a frame. Fig. 4 shows the load-deflection diagram of numerical results and the Vogel results (Vogel 1985).

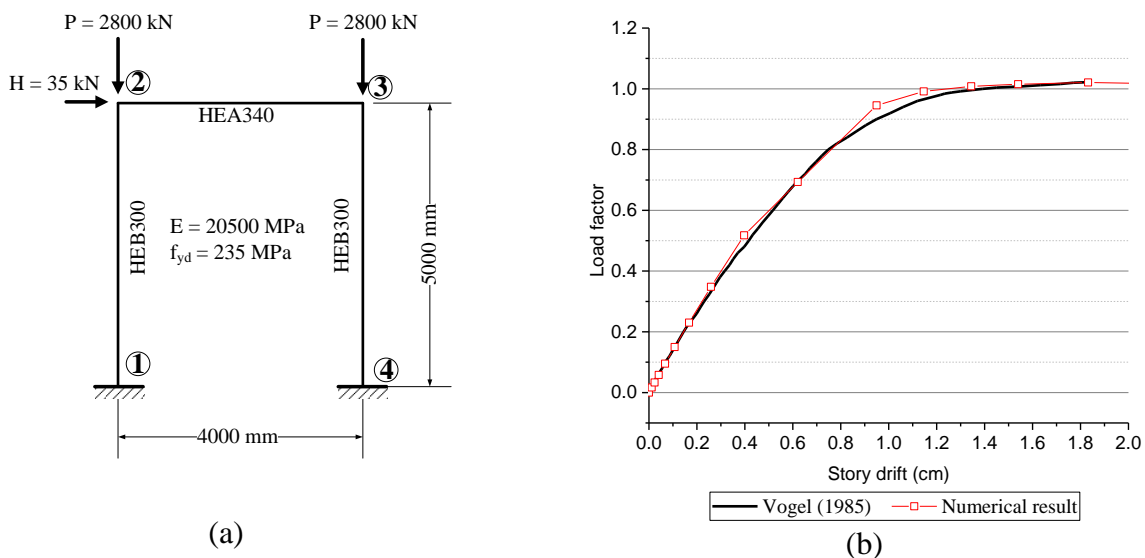


Figure 4: (a) Studied Vogel's portal and (b) the load-deflection diagram obtained.

The connections of steel storage pallets were modeled by torsional springs. “Join-Rotational” method was used to represent the connection behaviors. The validation of BCC was carried out using nonlinear curve moment-rotation of Zhao et al. 2014 (C3-B105-4T curve). Similarly, the validation of base-plate connections used the curves moment-rotation of Godley, Beale and Feng 1998. However, the results of Godley, Beale and Feng 1998 were not used in this study, since the profiles used are different from those used by Zhao et al. 2014. Thus, the base connections are modeled by linear behavior described according to the moment-rotation relation defined by Sarawit and Peköz 2002. Eq. 1 shows the moment-rotation relation defined by Sarawit and Peköz 2002.

$$M = \left(\frac{7}{20} b d^2 E_c \right) \theta \quad (1)$$

where b is the width of the column parallel to the flexural axis, d is the depth of the column perpendicular to the flexural axis and E_c is the modulus of elasticity of the concrete floor assumed according to Sarawit and Peköz 2002 equal to 20340 MPa.

Since the FE model was able to predict the: (i) strength of isolated members, (ii) frame behavior and (iii) the behavior of linear and non-linear connections, the authors considered the methodology presented as appropriate to predict the steel storage pallet rack stability analysis.

2.3 Steel Storage Pallet Racks evaluated

After the validation stage, it was possible to develop the advanced analysis model of the steel storage pallet rack. The FE model of the advanced analysis was characterized by a 3D model with: (i) open-section beam elements (B32OS) in order to capture torsional-flexural buckling mode and warping behavior of the open-section columns, as performed by Rasmussen and Gilbert 2010; (ii) beam elements (B32) to elements of pallet beams; (iii) linear torsional springs to model the connection stiffness of base-plate connections; (iv) nonlinear torsional springs to model the BCCs. The FE models consider both geometric and material nonlinearities of steel pallet racks. Fig. 5 shows the models created to carry out the advanced analysis. It also shows the comparison of the advanced analysis model with the models referring to AISI and RMI standards, which will be explained in the next section.

The initial geometrical imperfections were taken in account directly in advanced analyses. Out-of-plumbness (Δ) is defined by coordinates of the nodes and the out-of-straightness (δ) is defined by preliminary static analysis defined with uniform loads. The uniform loads were defined in order to generate the desired deflection. The amplitude of the imperfections was defined by the assembly limits as reported in the RMI MH16.1:2012. The maximum top to bottom out-of-plumb ratio accepted and adopted is 1/240 as well as the maximum out-of-straight ratio is 1/240. Note that, Fig. 5 shows the imperfection configuration adopted in this work; note this is not necessarily the worst possible imperfection shape.

Note that, the non-linear problem of advanced analysis was solved by Riks method in order to obtain the maximum capacity of the structure. The load applied in the AISI and RMI analyses was obtained by multiplying the load applied in the advanced analysis by the peak load value.

Thus, the results from the three analyses (advanced analysis, AISI and RMI) are respective to the same applied load.

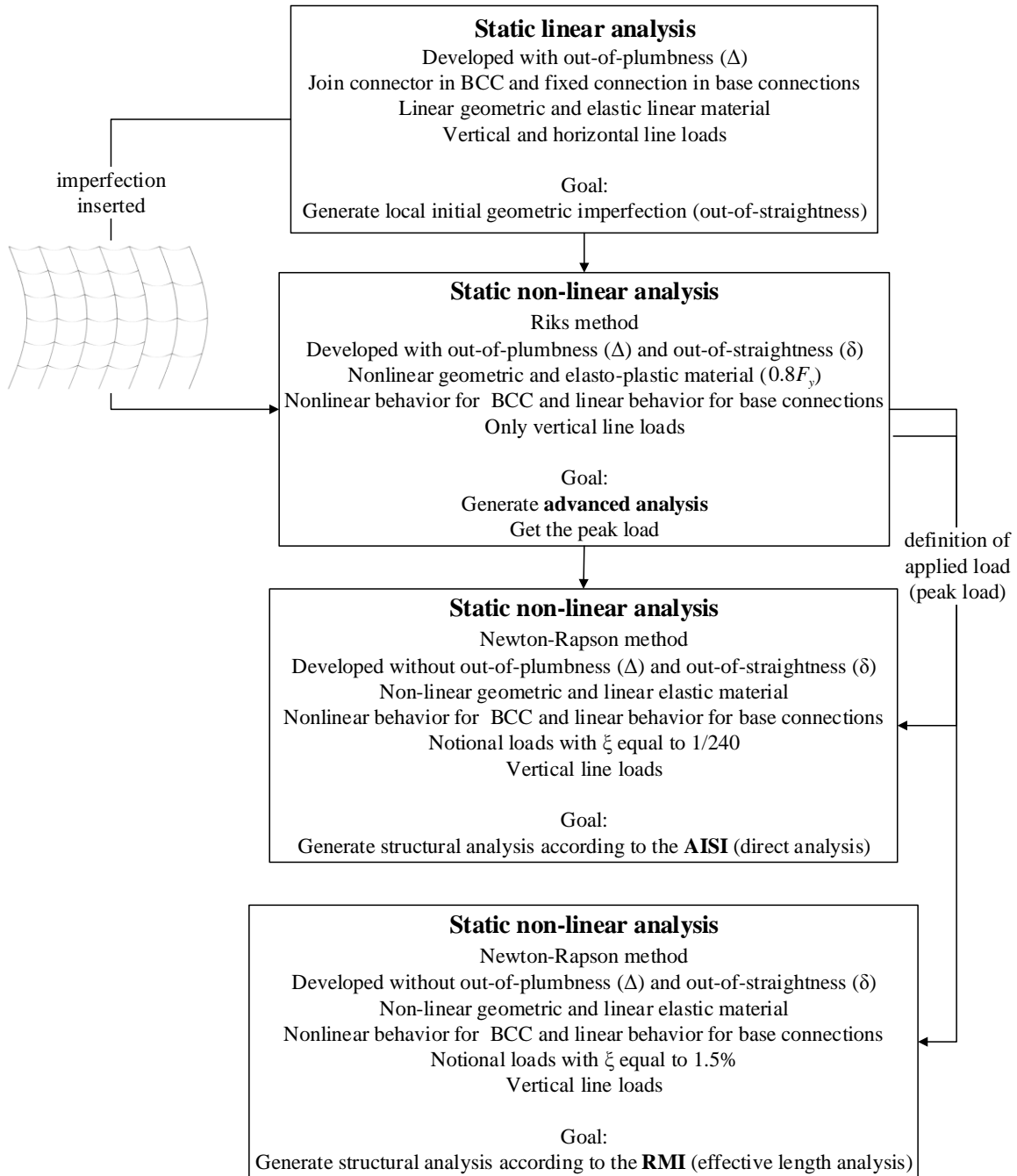


Figure 5: Steps to make an advanced analysis and the models to compare the design standards.

The analysis of steel storage pallet racks were carried out using Abaqus Scripting and Python.

3. Comparison of design standards

In this section, racks are analyzed by the specifications RMI MH 16.1:2012 and ANSI/AISI S100-16. The design codes are compared using the M-N interaction equation results obtained

from the critical column of the rack. Hence, Eq. 2 was used as an interaction equation for results of advanced analysis.

$$\frac{\bar{P}}{0.80A_g F_y} + \frac{\bar{M}}{0.80S_{fy} F_y} \leq 1.0 \quad (2)$$

where \bar{P} and \bar{M} are required compressive axial strength and required flexural strength obtained from advanced analysis at peak load, A_g is the gross area of the column, S_{fy} is the elastic section modulus of full unreduced cross-section relative to extreme fiber in first yielding and, finally, F_y is the nominal yield stress of columns. Note that, the adopted safety factors are equal to value used in static linear analysis showed in Fig. 5. ANSI/AISI S100-16 recommends the value equal to 0.80 as safety factor to rational engineering analyses, such as advanced analyses.

3.1 ANSI/AISI S100-16

Fig. 5 showed the structural analysis requirements of ANSI/AISI S100-16 used in this study. Note that a perfect structure was evaluated (i.e. without initial geometric imperfections) with notional loads applied at all levels with magnitude N_i as shown in Eq. 3:

$$N_i = \xi Y_i \quad (3)$$

where Y_i is the gravitational load applied at level i and ξ is the factor equal to 1/240 according ANSI/AISI S100-16. The design of this analysis is based on direct analysis approach, i.e., considering K equal to unity. Eq. 4 shows the interaction equation used for both design codes.

$$\frac{\bar{P}}{0.85P_{ne}} + \frac{\bar{M}}{0.90M_{ne}} \leq 1.0 \quad (4)$$

where \bar{P} and \bar{M} are required compressive axial strength and required flexural strength, respectively, obtained from elastic second order analysis, P_{ne} and M_{ne} are the nominal axial strength and the nominal flexural strength, respectively, using actual member length for the flexural buckling and torsional buckling verifications. Herein, the adopted safety factors are 0.85 to members in compression and 0.90 to members in flexure according ANSI/AISI S100-16.

3.2 RMI MH 16.1:2008

The structural analysis using RMI is similar to AISI requirements. The fundamental difference is in the value of the factor ξ . The story drift ratio ξ in the RMI analysis is equal to 1.5%.

In the context of design, based on effective length method, RMI MH 16.1:2008 indicates that pallet racks with semi-rigid connections will have K values greater than 1.0 and may even exceed 2.0 to flexural buckling design in the direction perpendicular to the upright frame. RMI MH 16.1:2008 allows the use of K equal to 1.7 as a default value that represents an average

value. For flexural buckling in the plane of the upright frame, the effective length factor can be taken as 1.0 and, finally, the value of K_t is taken equal to 0.8 (RMI MH 16.1:2008).

Sarawit and Peköz 2006a indicate that the recommended value of K taken as one to the flexural buckling in the upright plane is in general conservative while the value 0.8 to the K_t is reasonable since there is adequate braces and the column base is constrained against twisting. According to the same authors, the assumption of constrained base against twisting is valid because of the presence of the anchorage bolts in the connection and the friction effects between the steel base plate and concrete floor.

In this study, the authors considered: (i) K equal to 1.7 to flexural buckling in the direction perpendicular to the upright frame; (ii) K equal to unity to the flexural buckling in the upright plane and, finally, (iii) K_t equal to 0.8. These values are used in the interaction equation, Eq. 4.

3.3 Perforated steel storage racks studied

Herein, the applicability of the design standards applied to irregular racks was evaluated as shown in Fig. 6. This type of steel pallet rack is an alternative for the storage of products with different heights generating different loading.

Fig. 6 shows the typical racks evaluated in this paper. Three 6-storey unbraced racks with two floor heights (h_1 and h_2) were studied. The terms nb_1 and nb_2 indicate the number of bays defined in each region: region where the floor height is equal to h_1 ("Region H1") or region where the floor height is equal to h_2 ("Region H2"). The values adopted in this study were: h_1 and h_2 equal to 1450 mm and 2175 mm, respectively and L_b equal to 1860 mm. In addition to the floor height difference, each region can also be loaded with different load values.

Only vertical uniform loads were applied in the stories in the Region H1 and in the Region H2. It can be assumed that each shelf beam is loaded by a uniform load (force per length) because, in this paper, it is assumed that vertical loads are equally distributed over the entire bay.

Although only the down-aisle plane was modeled, the three-dimensional effects of columns and beams were captured. For this, the contour conditions showed in Fig.6 were defined based on assumptions about cross-aisle direction. Fig. 7 shows the hypotheses adopted in Regions H1 and H2. In addition, the boundary conditions were defined according to the literature (Rasmussen and Gilbert 2010 and Sarawit and Peköz 2006b).

Fig.8 shows the structural components used in this paper. For the columns, the "C3" cross-section of Zhao et al. 2014 was adopted. For the beams, the "B105" cross-section of Zhao et al. 2014 was used with small adjustments in order to use a doubly-symmetrical section; these adjustments were necessary because the authors believed that torsional loads due to section asymmetry would lead to additional work without adding any substantial conclusion.

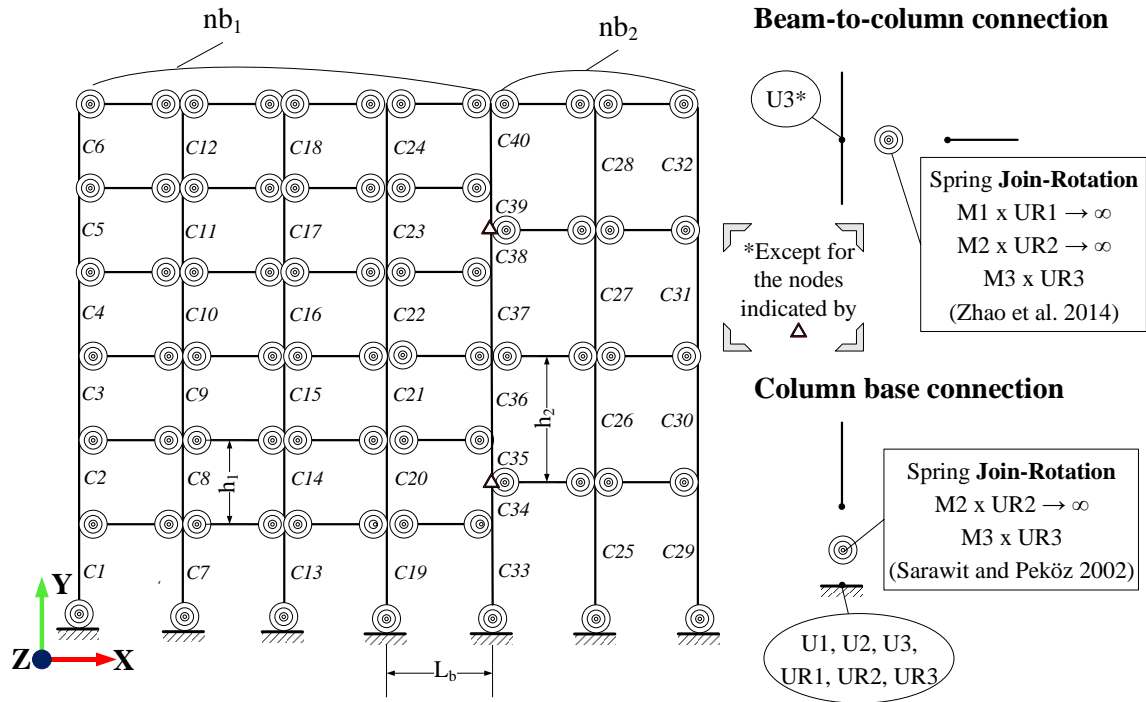


Figure 6: Typical rack evaluated in the paper.

Hypotheses assumed for the cross-aisle direction

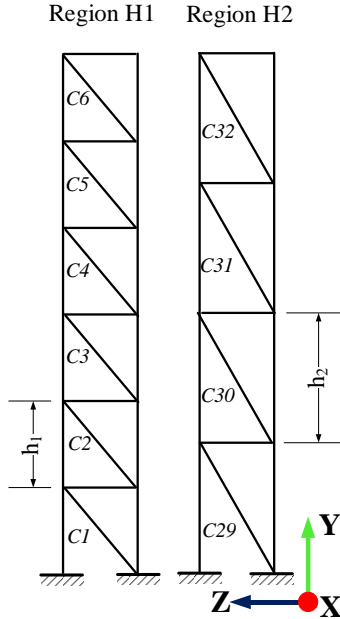


Figure 7: Upright frames adopted in Regions H1 and H2.

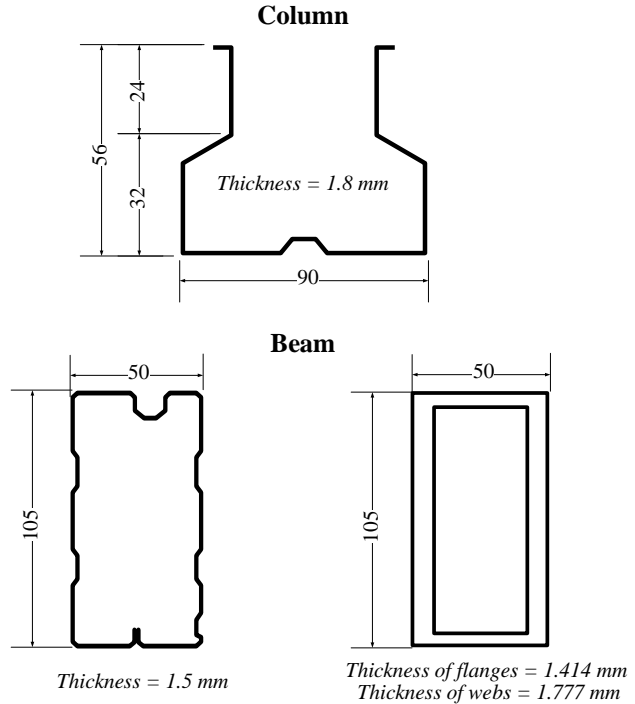


Figure 8: Cross-section of the column and cross-sections of the beam: the original (left hand side) and the adopted in this study (right hand side).

Tables 2 and 3 summarize the results of the critical column using direct analysis and effective length methods. The values of the second-order drift and the first-order drift were taken from the upper right node.

Table 2: Results of AISI analysis of the critical column and its design using direct analysis method.

Rack		Applied uniform load (kN/cm)				Interaction equation results		
nb1	nb2	$\frac{\text{Load H1}}{\text{Load H2}}$	Region H1	Region H2	$\frac{\Delta_{2\text{nd order}}}{\Delta_{1\text{st order}}}$	Advanced Analysis (critical column)	ANSI/AISI S100:2010 (critical column)	Relative error (%)
							Region H2	
4	2	1	0.060145	0.060145	1.029	1.038992 (C33) Between Region H1 and H2	1.312718 (C25) Region H2	26.3453
4	2	2.5	0.065883	0.026353	1.628	0.958070 (C33) Between Region H1 and H2	1.144401 (C19) Region H1	19.4486
4	2	5	0.067559	0.013512	1.528	0.961352 (C19) Region H1	1.170786 (C13) Region H1	21.7854

Table 3: Results of RMI analysis of the critical column and its design using effective length method.

Rack		Applied uniform load (kN/cm)				Interaction equation results		
nb1	nb2	$\frac{\text{Load H1}}{\text{Load H2}}$	Region H1	Region H2	$\frac{\Delta_{2\text{nd order}}}{\Delta_{1\text{st order}}}$	Advanced Analysis (critical column)	RMI MH16.1:201 2 (critical column)	Relative error (%)
							Region H1	
4	2	1	0.060145	0.060145	1.337	1.038992 (C33) Between Region H1 and H2	1.519762 (C25) Region H2	46.2727
4	2	2.5	0.065883	0.026353	1.715	0.958070 (C33) Between Region H1 and H2	1.208332 (C19) Region H1	26.1215
4	2	5	0.067559	0.013512	1.525	0.961352 (C19) Region H1	1.236222 (C13) Region H1	28.5921

As expected, the maximum axial force and bending moment values were found between the base and the first beam level and the critical M-N combinations were also found for the columns between the base and the first beam levels. However, the critical columns of the AISI and RMI procedures were not equal to those obtained in the advanced analysis, but they were similar when compared to each other.

The change in the value of the LoadH1/LoadH2 ratio generated different values of $\Delta_{2\text{nd order}}/\Delta_{1\text{st order}}$ ratio. The LoadH1/LoadH2 case equal to 5.0 generates a ratio value equal to the limit defined by AISI for the applicability of the effective length method. On the other hand, LoadH1/LoadH2 equal to 2.5 leads to a ratio value not acceptable by the effective length method.

Regarding the load-carrying capacity, Tables 2 and 3 show that the increase in the value of the uniform load in the Region H2 does not imply that a significant change in the loading capacity of Region H1.

Tables 2 and 3 also show conservatism reduction for increasing the LoadH1 / LoadH2 ratio from 1 to 2.5. The reduction in conservatism of the RMI method was greater than that observed by the AISI method. Namely, the effective length method was more sensitive to the loading variations than the direct analysis method. Fig. 9, 10 and 11 show the interaction equation results for all columns shown in Fig. 6.

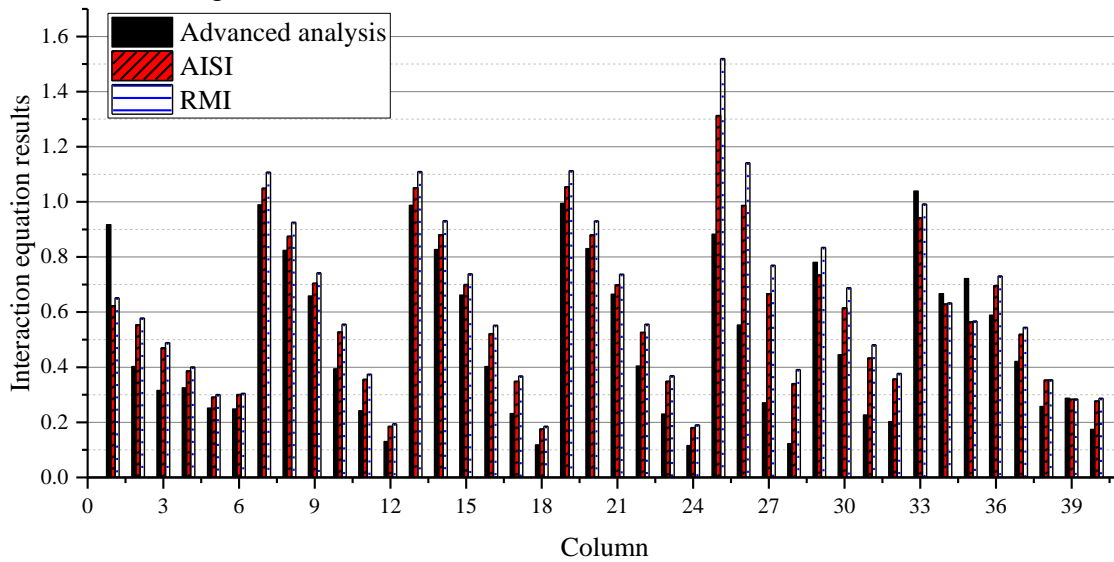


Figure 9: Comparison of design methods for the stability analysis of the rack with equal values of vertical uniform load (LoadH1 / LoadH2 = 1.0).

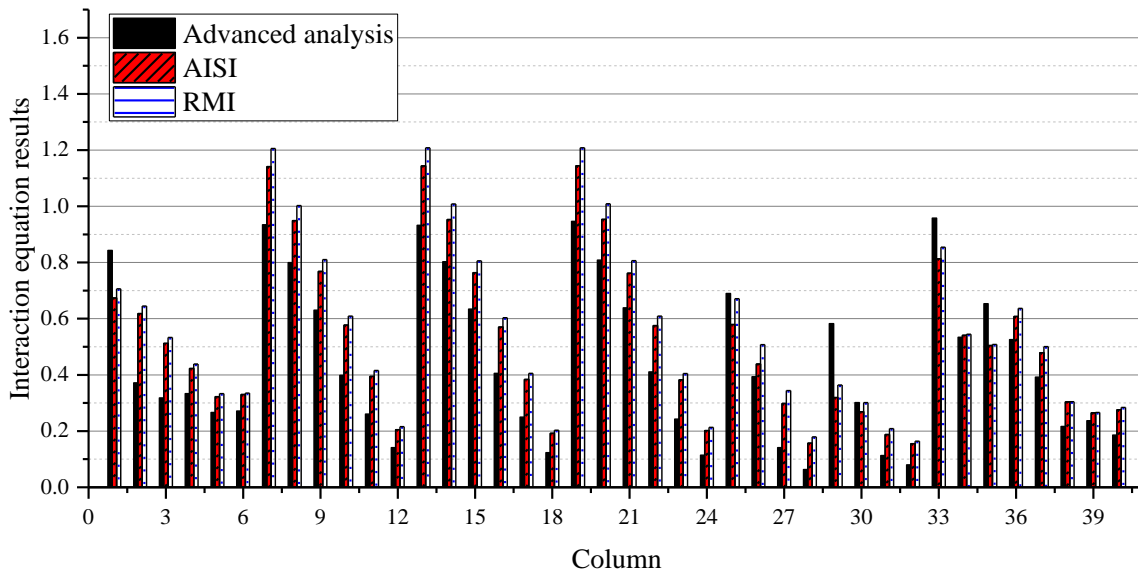


Figure 10: Comparison of design methods for the stability analysis of the rack with LoadH1 / LoadH2 equal to 2.5.

Fig. 9, 10 and 11 depicted that for most columns both the current design methods are conservative. However, in all three cases, there are columns with non-conservative results of RMI and AISI, i.e., there are interaction expression results smaller than those obtained in the advanced analysis.

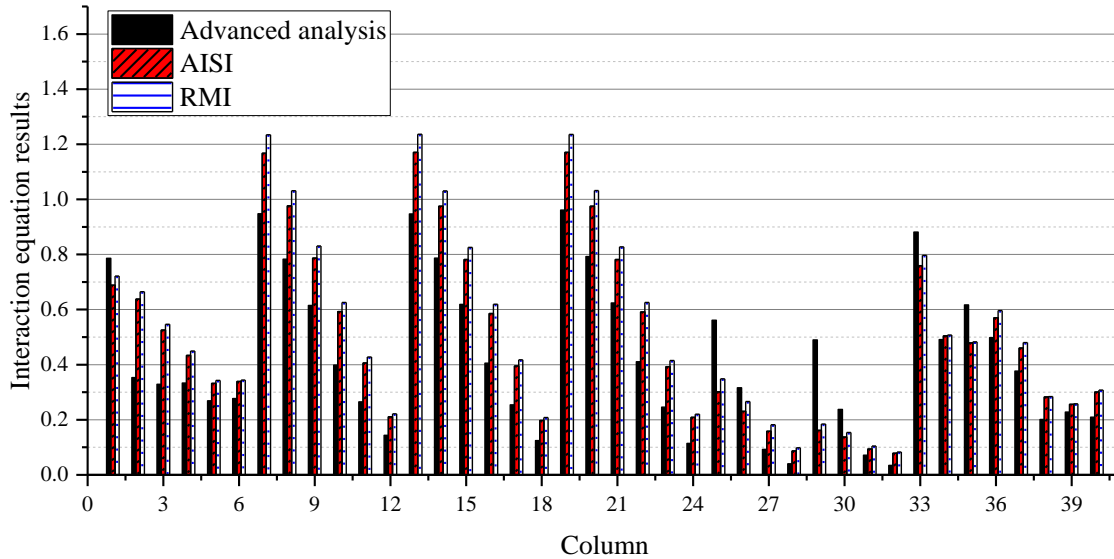


Figure 11: Comparison of design methods for the stability analysis of the rack with LoadH1 / LoadH2 equal to 5.0.

As observed by Sarawit and Peköz 2006b, the notional load method better represent finite element results than the effective length method does. In addition, the irregular geometry of the rack showed the importance of loading on Regions H1 and H2.

4. Lattice model

Since beam element models are not able to predict local and distortional buckling modes, an alternative model is proposed. Advanced analysis of cold-formed members is usually performed using finite shell elements to assess the effects of cross-sectional buckling modes. However, the use of shell elements limits the numerical analysis due to the high computational cost especially in complex and perforated members. Thus, the overall frame model leads to great computational cost.

Herein, an alternative method using one-dimensional finite elements (truss and beams elements) was presented. Fig 12 shows the proposed method. Note that the following resources were used: (i) a free program Gmsh (Geuzaine and Remacle 2009) to mesh the shell model; (ii) Python language to create a code that manipulates the mesh, and finally (iii) Abaqus software to perform the FE analysis.

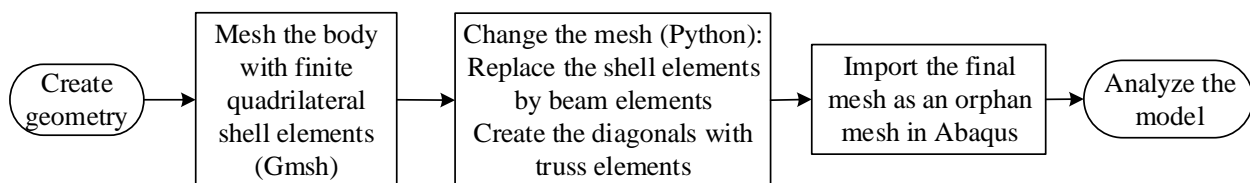


Figure 12: Applied methodology to create lattice models.

Fig 13. presents the methodology for the case of the isolated shell $B \times L$ with fixed base submitted to uniform compression. The deformed shapes are the result of elastic stability analysis and second-order analysis.

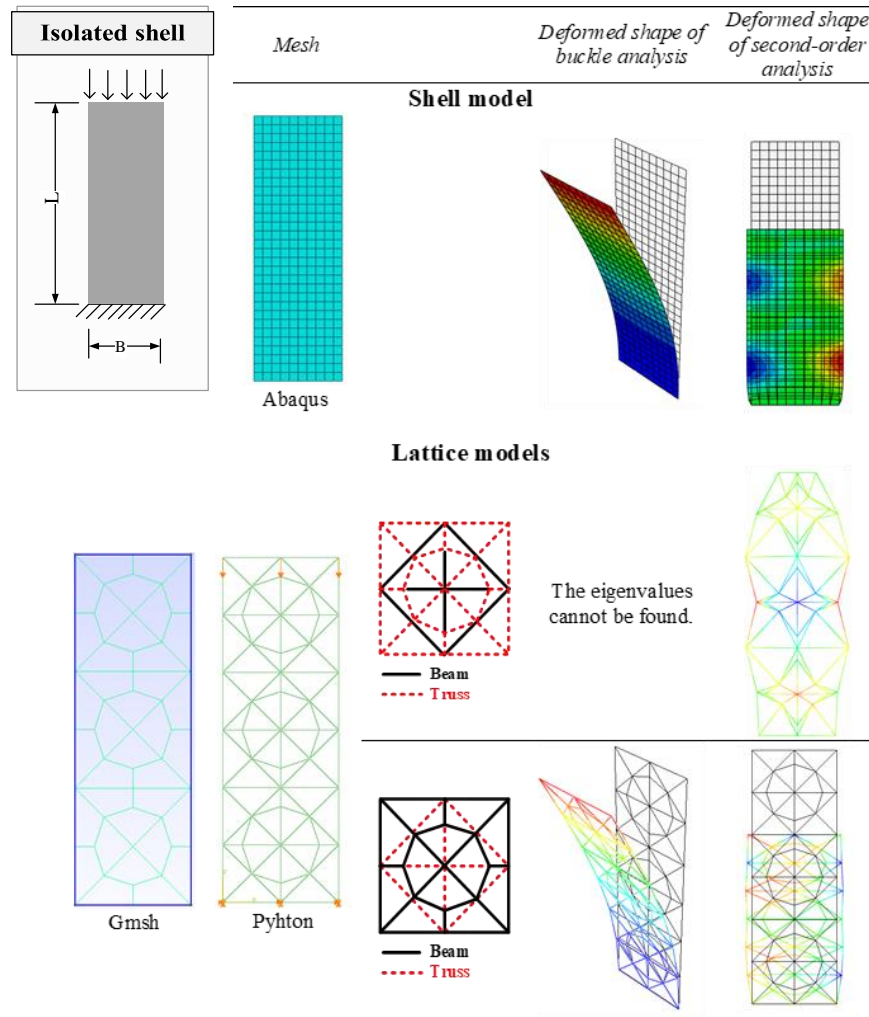


Figure 13: Isolated shell evaluated by shell model and lattice models.

To clarify the construction of the lattice models, Fig. 13 shows the deformed shape of a shell element model with two element discretization. One can note that if shell elements are substituted by truss elements and diagonals by beam elements the results are not similar to the shell element results. On the other hand, the composition presented in Fig.12 (shell elements are substituted by beam elements with diagonals by truss elements) results agree with shell element model and lead to lower computational cost.

Thus, the methodology described in Fig. 12 was adopted and element B31 was used for the beam elements and T3D2 for the truss elements.

4.1 Perforated steel storage racks columns

In the context of advanced analysis, the consideration of features of CFS profiles is fundamental at least to the columns design. Columns are usually singly symmetric, cold-formed, open

perforated sections, susceptible to local and distortional buckling modes. In this paper, the mechanical behavior of a column is evaluated through the lattice model approach considering all these characteristics.

The column used as reference in this study was taken from the work of Elias et al. 2018. Fig. 14 shows the model used. The boundary conditions were applied according to Elias et al. 2018 in order to represent the tests performed by them. In their numerical study, Elias et al. 2018 opted to restrict only the nodes that define the geometry of the profile, which are reproduced in this study by restrict the nodes directly (top end) and using a reference point (bottom end). F1, F2 and W are the points at half height of the member that Elias et al. 2008 instrumented with LVDTs.

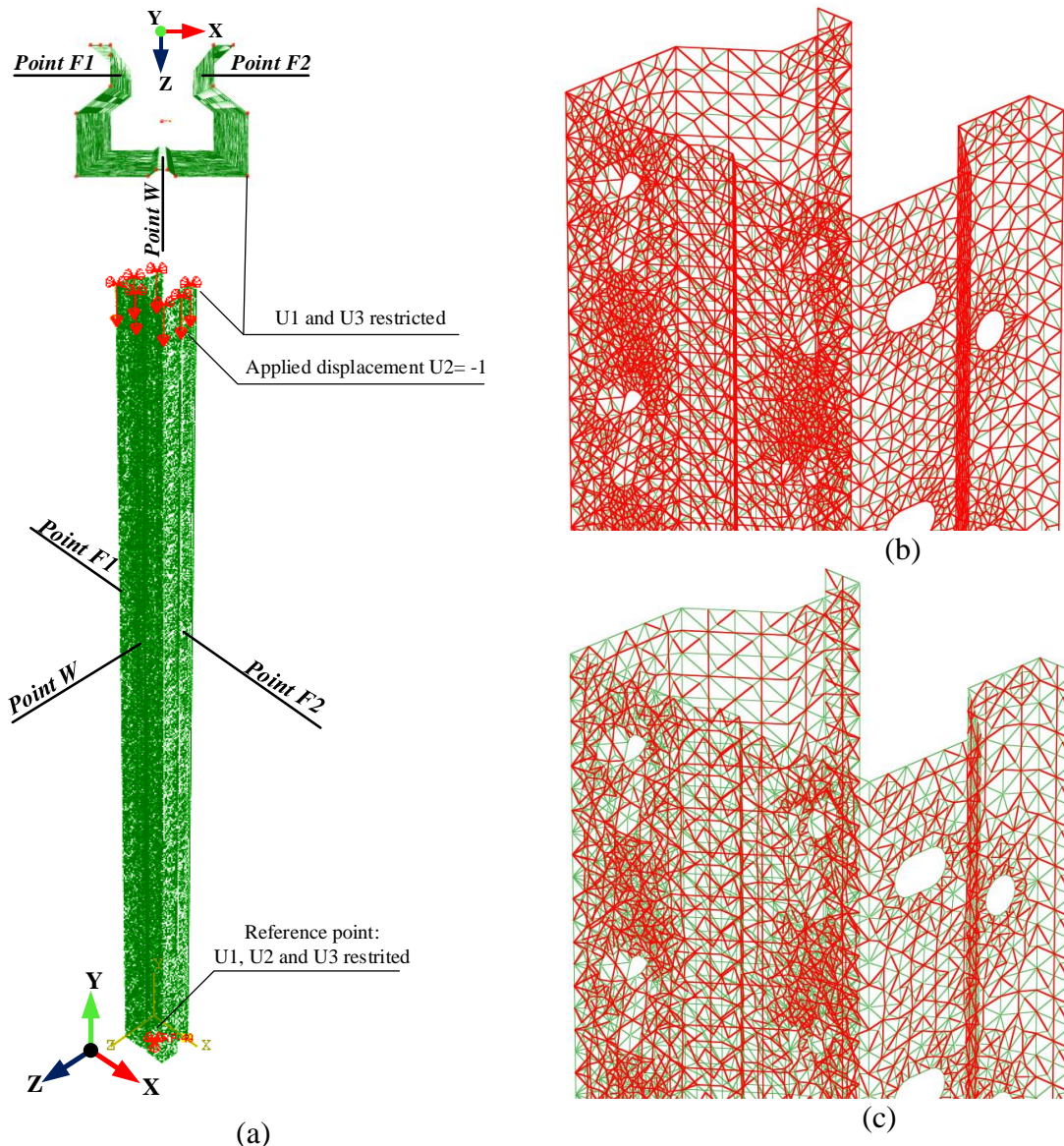


Figure 14: (a) Model evaluated by lattice model: (b) the beam elements are highlighted (red color) and (c) the truss elements are highlighted (red color).

Defining the profiles of the beam and truss elements is not a trivial task in lattice models. Hence, a parametric study was carried out to understand the influence of the area of the beam and truss elements that leads to the best combination of cross-sections to determine the column strength. Fig.15 and Table 4 summarize the results of the analysis. The relative errors presented are calculated using as a reference the results reported in Elias et al. 2018. Fig. 15 and Table 4 summarize the results of the analyses in terms of strength and failure modes, respectively.

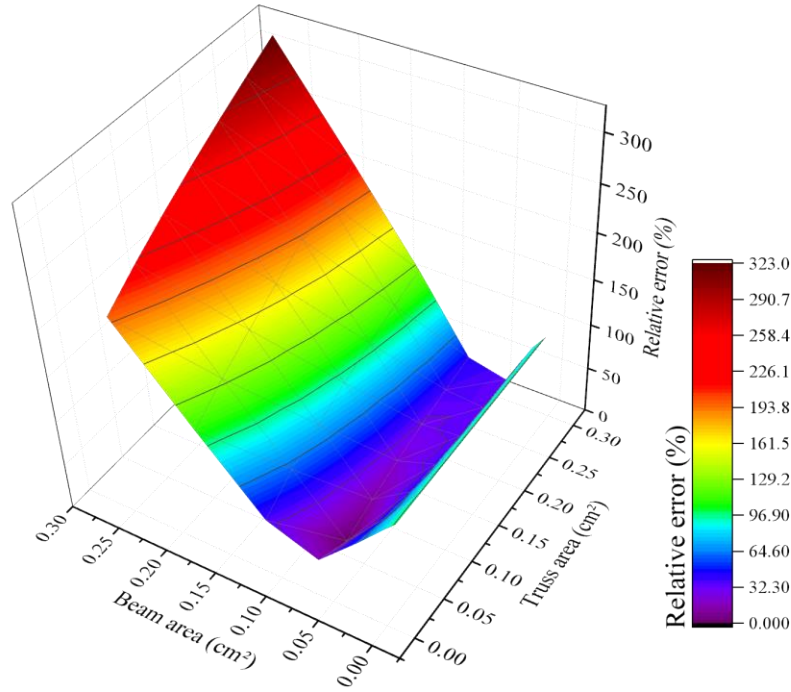


Figure 15: Relative errors of column strength varying cross-section of FE.

Table 4: Failure modes observed in analysis by lattice model for case I.

Beam area (cm ²)	Truss area (cm ²)						
	0.020	0.065	0.110	0.155	0.200	0.245	0.290
0.001	L+D	L	L+d	L+d	L+D	L+d	D
0.013	D	FT+D	FT+D	FT+D	FT+D	FT	FT+d
0.038	F1/FT	F1/FT	F1/FT	FT+d	FT+D	FT+D	FT+D
0.075	F2+d	F1/FT	F1/FT	F1/FT	F1/FT	F1/FT	FT
0.126	F2+D	F2+D	F1/FT	F1/FT	F1/FT	F1/FT	FT
0.189	F2+d	F2+d	F2	F2	F2	F1/FT	FT
0.264	F2+d	F2+d	F2	F2	F2	F2	F2

Main effect	Failure modes	Second effect
D	Distortional	d
L	Local	l
F1/FT	Flexural mode about strong axis (F1) coincident with flexural-torsional mode (FT)	f1/ft
F2	Flexural mode about weak axis	f2
FT	Flexural-torsional mode	ft

The results of the parametric study showed in Fig. 15 indicate an optimal point that the relative numerical strength error was 0.4%.

Table 4 shows the behavior of failure modes as a function of the beam and truss areas. As expected, the cross-section buckling modes are associated with lower area values and the global modes are associated with higher area values.

The validation in terms of failure mode was carried out by comparing the numerical displacements with the LVDTs results. Fig. 16 shows the results of the optimal point of Fig. 15 comparing with experimental results. Fig. 17 shows the deformed configuration of these member under the peak loading.

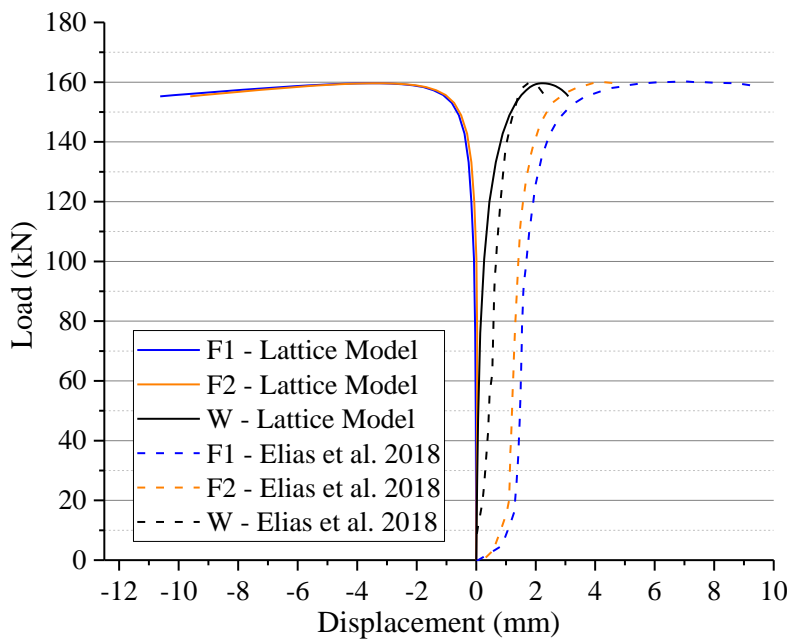


Figure 16: Behavior of column strength comparing with experimental results of Elias et al 2018.

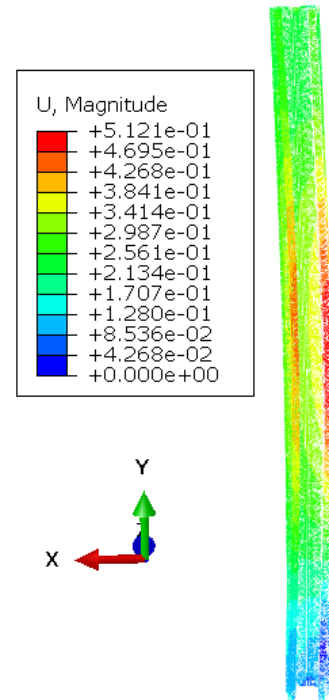


Figure 17: Displacement filed of column at peak load (values in centimeters).

The results showed in Fig. 16 and 17 are from the optimal point obtained in Fig. 15: truss area equal to 0.065 cm² and beam area equal to 0.075 cm².

5. Conclusions

A study comparing the effective length method and the direct analysis method for irregular CFS storage rack design was carried out. Three loading conditions were evaluated. These models take in account geometric and material nonlinearities, initial geometric imperfections, non-linear connection behavior and three-dimensional behavior of columns.

For the frames studied, both procedures (AISI and RMI) were conservative. Among them, it is recommended that the notional load method be considered as an alternative means for industrial

steel storage rack design. The direct analysis method was less conservative and less sensitive to loading variations.

However, the conclusions previously summarized neglect the local and distortional buckling modes. To capture all these effects, the lattice model methodology has shown to be promising and may lead to an advanced cold-formed steel analysis. Lattice model approach proved to be efficient when combining truss and beam elements to reduce computational cost. For this, a parametric study is necessary varying the cross sections of the elements in order to obtain the situation that satisfies both the required ultimate strength and the required failure mode.

Acknowledgments

This study was financed in part by the Coordenação de Aperfeiçoamento de Pessoal de Nível Superior (CAPES), Finance Code 001 and by the National Council for Scientific and Technological Development, CNPq, (Process number 140458/2017-4). Financial supports are gratefully acknowledged.

References

- American Institute of Steel Construction (2010). ANSI/AISC 360. "Specification for Structural Steel Buildings." Chicago, Illinois.
- American Institute of Steel Construction (2016). ANSI/AISC 360. "Specification for Structural Steel Buildings." Chicago, Illinois.
- American Iron and Steel Institute (2016). ANSI/AISI S100. "North American Specification for the Design of Cold-Formed Steel Structural Members." Washington, D.C..
- American Society of Civil Engineers (1997). "Effective Length and Notional Load Approaches for Assessing Frame Stability: Implications for American Steel Design", Task Comitee on Effective Length, ASCE, New York, N.Y..
- Cardoso, F.S., Rasmussen, K.J.R. (2016). "Finite element (FE) modelling of storage rack frames" *Journal of Constructional Steel Research*, 126, 1-14.
- Cold-Formed Steel Structures. (2005). AS/NZS 4600, Standards Australia, Sydney.
- Dória, A.S., Malite, M., Vieira Jr., L.C.M. (2013). "On Frame Stability Analysis" *Proceedings of the Annual Stability Conference Structural Stability Research Council*, St. Louis, Missouri.
- Elias, G.C., Neiva, L.H.A., Sarmanho, A.M.C., Alves, V.N., Castro, A.F.B. (2018) "Ultimate load of steel storage systems uprights" *Engineering Structures*, 170, 53-62.
- Galambos, T.V., Ketter, R.L. (1959). "Columns under Combined Bending and Thrust." *Journal of the Engineering Mechanics Division*, ASCE, 85, no. EM2, 1-30.
- Geuzaine, C., Remacle, J.-F. (2009) Gmsh: a three-dimensional finite element mesh generator with built-in pre- and post-processing facilities. *International Journal for Numerical Methods in Engineering*, 79(11), 1309-1331.
- Gmsh. Free program available in < <http://gmsh.info/> >.
- Godley, M.H.R., Beale, R.G., Feng, X. (1998) "Rotational stiffnesses of semi-rigid baseplates" *Proceedings of the Fourteenth International Specialty Conference on Cold-Formed Steel Structures*, St. Louis, Missouri U.S.A.
- Lavall, A.C.C., Silva, R.G.L., Costa, R.S, Fakury, R.H. (2013). "Advanced analysis of steel frame using the Brazilian Standard" *Revista da Estrutura de Aço*, 2 (3) 146-165.
- Rack Manufacturers Institute. (2008). "Specification for the Design, testing and Utilization of Industrial Steel Storage Racks". Charlotte (USA): Rack Manufactures Institute.
- Rack Manufacturers Institute. (2012). "Specification for the Design, testing and Utilization of Industrial Steel Storage Racks". Charlotte (USA) : Rack Manufactures Institute.
- Rasmussen, K.J.R., Gilbert, B.P. (2010) "Analysis-based 2D design of steel storage racks." *Research Report R908*, School of Civil Engineering, The University of Sydney, Sydney, Australia.
- Rasmussen, K.J.R., Gilbert, B.P. (2013). "Analysis-Based Design Provisions for Steel Storage Racks" *Journal of Structural Engineering*, 139 (5) 849-859.
- Sarawit, A.T., Peköz, T. (2002). "Design of industrial storage racks" *Proceedings of Sixteenth International Specialty Conference on Cold-Formed Steel Structures*, Orlando, Florida USA, 369-384.

- Sarawit, A.T., Peköz, T. (2006a). "Cold-Formed Steel Frame and Beam-Column Design." *Research Report RP03-2*, Committee on Specifications for the Design of Cold-Formed Steel Structural Members.
- Sarawit, A.T., Peköz, T. (2006b). "Notional load method for industrial steel storage racks." *Thin-Walled Structures*, 44, 1280-1286.
- Steel Storage Racking, AS 4084, Standards Australia, Sydney, 2012.
- Trouncer, A.N., Rasmussen, K.J.R. (2016a). "Ultra-light gauge steel storage rack frames. Part 1: Experimental investigations" *Journal of Constructional Steel Research*, 124, 57-76.
- Trouncer, A.N., Rasmussen, K.J.R. (2016b). "Ultra-light gauge steel storage rack frames. Part 2 – Analysis and design considerations of second order effects" *Journal of Constructional Steel Research*, 124, 37-46.
- Vogel, U. (1985). "Calibrating Frames" *Stahlbau*, 10, 295-301.
- Zhao, X., Wang, T., Chen, Y., Sivakumaran, K.S. (2014) "Flexural behavior of steel storage rack beam-to-upright connections" *Journal of Constructional Steel Research*, 99, 161-175.